SPACE TELESCOPE SCIENCE INSTITUTE
Operated for NASA by AURA

Instrument Science Report STIS 2011-01(v1)

Wavelength Calibration Accuracy for the STIS CCD and MAMA Modes

Ilaria Pascucci[1], Phil Hodge[1], Charles R. Proffitt[1] & T. Ayres[2]

[1] Space Telescope Science Institute, Baltimore, MD 21218
[2] University of Colorado, Boulder, CO 80309-0389

March 29, 2011

ABSTRACT

Two calibration programs were carried out after Servicing Mission 4 to determine the accuracy of the wavelength solutions for the most used STIS CCD and MAMA modes. We report here on the analysis of this dataset and show that the STIS wavelength solution has not changed after SM4. We also show that a typical accuracy for the absolute wavelength zero-points is 0.1 pixels while the relative wavelength accuracy is 0.2 pixels.

Contents

Introduction

The Space Telescope Imaging Spectrograph (STIS, Kimble et al. 1998) operated on-orbit from February 1997 until a malfunction in August 2004. During Hubble Servicing Mission 4 (SM4), STIS was successfully repaired and resumed operations in May 2009. To allow the wavelength scale for individual science observations to be corrected for non-repeatability and drifts in the STIS optical element alignment, most observations of external targets are accompanied by one or more wavelength calibration spectra. There are three Pt/Cr-Ne lamps on STIS for this purpose. These lamps are designated LINE, HITM1, and HITM2. The LINE lamp is located on the Insertion Mechanism platform. When the lamp is used, the Calibration Insert Mechanism (CIM) is placed into the light path and all external light is blocked. The HITM1 and HITM2 lamps are located on the Hole In The Mirror platform and can be used both for wavelength calibration and target acquisition (though the HITM2 lamp is considered the spare lamp and has not been used for target acquisition). The LINE lamp, being the brightest of the 3 Pt/Cr-Ne lamps, is being used for the least sensitive modes on STIS, especially the FUV echelle modes. The optics of the HITM1 and HITM2 lamps are such that their lower flux on the detector is more suited for the wavelength calibration of more sensitive modes on STIS, such as the optical low-resolution modes.

In order to test whether there has been any change in the wavelength solution post-SM4, we have obtained internal wavelength exposures covering many CCD and MAMA modes, focusing primarily on those used in GO programs as well as those utilized in previous calibration programs. This study measures the wavelength difference between lines in the STIS spectra and reference lines from a catalogue. It shows that the STIS wavelength solution has not changed after SM4 and that the accuracy is typically within 0.2 pixels.

Data

Wavelength calibration exposures have been obtained for many STIS CCD and MAMA modes frequently used both in GO programs as well as in previous calibration programs. The CCD exposures, which cover 39 different modes, were taken under program PID 11858 while the MAMA exposures, covering 26 different modes, were taken under program PID 11859. CCD lamp spectra were acquired with the $52 \times 0.1''$ slit and exposure times ranged from 4 to over 200 s. MAMA lamp spectra were obtained with varying small apertures ranging from $0.2 \times 0.06''$ in the echelle modes to $52 \times 0.1''$ in the first-order spectroscopic modes. A summary of the observations can be found in Tables 1 and 2.

To compare the line spectra with catalogued Pt/Cr-Ne lines we used the original compilation from Don Lindler as well as new compilations of Pt/Cr-Ne lines from the

NIST database[1], Sansonetti et al. (2004) for wavelengths <1830 Å and of Cr I lines from Wallace & Hinkle (2009) in the NUV portion of the STIS band (λ >2200 Å).

Spectral Element	Central Wavelength [Å]	Aperture [″]	Lamp	Time [s]
G230LB	2375	52X0.1	HITM1	220.0
G230MB	1713	52X0.1	HITM1	368.0
G230MB	2135	52X0.1	HITM1	30.0
G230MB	2276	52X0.1	HITM1	84.0
G230MB	1854	52X0.1	HITM1	600.0
G230MB	2416	52X0.1	HITM1	41.0
G230MB	2557	52X0.1	HITM1	63.0
G230MB	1995	52X0.1	HITM1	190.0
G230MB	2697	52X0.1	HITM1	14.0
G230MB	2794	52X0.1	HITM1	30.0
G230MB	2836	52X0.1	HITM1	24.0
G230MB	2976	52X0.1	HITM1	10.0
G230MB	3115	52X0.1	HITM1	24.0
G430L	4300	52X0.1	HITM1	10.0
G430L	4300	52X0.1	LINE	10.0
G430M	3165	52X0.1	HITM1	10.0
G430M	3423	52X0.1	HITM1	10.0
G430M	3680	52X0.1	HITM1	10.0
G430M	3843	52X0.1	HITM1	10.0
G430M	3936	52X0.1	HITM1	13.0
G430M	4194	52X0.1	HITM1	17.0
G430M	4451	52X0.1	HITM1	18.0
G430M	4706	52X0.1	HITM1	21.0
G430M	4961	52X0.1	HITM1	24.0
G430M	5093	52X0.1	HITM1	10.0
G430M	5216	52X0.1	HITM1	10.0
G430M	5471	52X0.1	HITM1	26.0
G750L	7751	52X0.1	HITM1	6.2
G750M	5734	52X0.1	HITM1	5.9
G750M	6252	52X0.1	HITM1	4.1
G750M	6581	52X0.1	HITM1	4.1
G750M	6768	52X0.1	HITM1	3.9
G750M	7283	52X0.1	HITM1	3.9
G750M	7795	52X0.1	HITM1	29.0
G750M	8311	52X0.1	HITM1	10.0
G750M	8561	52X0.1	HITM1	10.0
G750M	8825	52X0.1	HITM1	10.0
G750M	9336	52X0.1	HITM1	10.0
G750M	9851	52X0.1	HITM1	220.0

Table 1. *Log of the observations from program PID 11858 (CCD)*

Analysis

We reduced the lamp exposures with CALSTIS as if they were science images. To do this we created a companion file (named oxxxxxxxx_wav.fits) and invoked this file as the argument of the keyword WAVECAL in the FITS header of the original file (named oxxxxxxxx_raw.fits). We also modified the keyword ASN_MTYP to SCIENCE so that the software treats the image as a normal science exposure and the WAVECAL keyword from OMIT to PERFORM. We further switched the keywords HELCORR (for the heliocentric correction) and FLUXCORR (for the flux calibration) to OMIT. For first-order spectroscopic modes, five spectra were extracted by summing 32 rows (EXTRSIZE keyword in CALSTIS equal to 32) from different locations on the flt image. The five spectra were centered on cross-dispersion locations 128, 320, 512, 704, 896. We used spectra from the middle of the chip (row 512) for the line identifications (see

[1]http://physics.nist.gov/PhysRefData/platinum/contents.html

Spectral Element	Central Wavelength [Å]	Aperture [″]	Lamp	Time [s]
E140M	1425	0.2X0.06	LINE	663.2
E140H	1526	0.2X0.09	LINE	300
E140H	1598	0.2X0.09	LINE	400.5
E140H	1234	0.2X0.09	LINE	550
E140H	1271	0.2X0.09	LINE	400
E140H	1343	0.2X0.09	LINE	550
E230M	1978	0.2X0.06	LINE	190.3
E230M	2415	0.2X0.06	LINE	135
E230M	2561	0.2X0.06	LINE	120
E230M	2707	0.2X0.06	LINE	87.2
E230H	1763	0.1X0.09	LINE	800
E230H	2013	0.1X0.09	LINE	500
E230H	2713	0.1X0.09	LINE	500
G140M	1218	52X0.1	LINE	450
G140M	1222	52X0.1	LINE	72.4
G140M	1321	52X0.1	LINE	72.6
G140M	1540	52X0.1	LINE	94.3
G140M	1420	52X0.1	LINE	75
G140M	1640	52X0.1	LINE	100
G140L	1425	52X0.1	LINE	140
G230M	1687	52X0.1	LINE	310.0
G230M	2338	52X0.1	LINE	40.0
G230M	2818	52X0.1	LINE	30.0
G230M	3055	52X0.1	LINE	22.0
G230L	2376	52X0.05	LINE	47.6
E230H	1963	0.1X0.09	LINE	800

Table 2. *Log of the observations from program 11859 (MAMA).*

next paragraph) and the spectra taken at different locations to check for bad pixels. The output of the CALSTIS pipeline is the x1d file, which contains wavelength, net count rate, error (sorted by order in case of echelle spectra). For echelle spectra a one-dimensional spectrum covering the full wavelength range of the mode was created by interleaving the flux-wavelength points in ascending wavelength order.

Following this approach, we created 65 1-D spectra covering all the grating-central wavelength combinations in programs 11858 and 11859 . Using a semi-automatic line identification routine written in IDL, we identified laboratory lines in the STIS spectra and computed the difference between the observed and catalogued lines for each grating-central wavelength combination. In order to verify our approach we also produced figures showing the identified lines on top of the STIS lamp spectra. The centroid pixel location for each line was measured in two ways: i) by fitting a gaussian to the lines, and ii) by computing a weighted mean using the counts over ± 2 pixels from the central one as a weighting factor. The errors on the centroid are the formal error on the peak of the gaussian for i) and the inverse of the square root of the counts over 5 pixels for ii). We then computed the mean and standard deviations of the differences per mode but also checked if there is any trend of the differences with wavelength within each mode.

CCD Modes

Our results on the wavelength accuracy of the CCD modes are summarized in Figs. 1–10. Fig. 4 shows that when the Wallace & Hinkle (2009) line compilation is not included there are many fewer lines for which the wavelength accuracy can be measured.

None of the CCD modes shows a wavelength dependence in the difference between observed and laboratory lines. The mean of the difference distribution is typically <0.1 pixel and the standard deviation is < 0.2 pixels as measured before SM4. In the two cases where standard deviations are $\sim$0.4 pixels (G230MB-2794 and G430M-3936), the large value is very likely due to the paucity of identified lines as shown for the G230MB modes when the Wallace & Hinkle (2009) compilation is not included.

MAMA Modes

Our results on the wavelength accuracy of the MAMA modes are summarized in Figs. 11–16. As noted for the CCD modes, including the Wallace & Hinkle (2009) compilation for those settings around 2300 Å increases the number of detected lines and hence gives more reliable estimates for the wavelength accuracy, see e.g. the E230H-2713 Å settings and several E230M settings.

We find that the high-resolution echelle settings (E140H and E230H) perform as pre-SM4: The mean of the difference distribution is typically <0.1 km/s (or 0.08 pixels) and the standard deviation is $\sim$0.3 km/s (or 0.2 pixels). These values are well in agreement with those reported in Ayres (2008) who used an independent approach to analyze deep (hundred seconds) high signal-to-noise wavecal exposures obtained before SM4. In a few instances, such as for the E230H-1963 Å setting, we see that higher order effects are not corrected by the current coefficients in the STIS dispersion relations. In the next section we report on tests that have been made using new coefficients and an expanded wavelength solution derived by Ayres using pre- as well as post-SM4 deep wavelength exposures. The medium resolution settings (E140M and E230M) have larger differences from laboratory wavelengths than the H settings, as expected from the lower spectral resolution. In pixels, the mean of the difference distribution is always less than 0.1 pixels while the standard deviation is typically <0.2 pixels but sometimes a bit larger up to 0.26 pixels. In these settings we see a few clear trends of offsets with wavelengths. Such trends have been independently identified by Ayres. We attempt to correct for them with the new and expanded wavelength solution (see next Section).

The MAMA G modes (medium and low resolution) perform as expected and as reported in the STIS Instrument Handbook. Specifically, the standard deviations between observed and laboratory wavelengths are between 0.15 and 0.5 pixels, with the G140L and G230L having the smallest deviations 0.2 pixels and 0.15 pixels respectively.

Further Improvements on the STIS Echelle Wavelength Accuracy

The current dispersion relations for the echelle modes produce some small but systematic offsets of the measured versus laboratory lines, see e.g. the E230H-1963 mode in Fig. 12. These offsets differ from one central wavelength to another. As part of two archival and one GO calibration programs (10203, 11743, and 12280) Tom Ayres has independently verified the accuracy of the STIS echelle modes and recently proposed

a modified version of the STIS dispersion polynomial which could further improve the wavelength accuracy (see Ayres 2010, HST calibration workshop). This new version includes two additional terms: one in $[m\,\lambda]^3$ and a second in m^2, where m is the echelle order number. In addition, he re-derived all dispersion coefficients for the CALSTIS pipeline polynomial using a more extensive set of lamp exposures obtained through the entire STIS lifetime. We tested this new dispersion relation with CALSTIS and found that while some improvements could be seen overall (e.g. for E230H-2013, see Fig. 17), a few modes presented larger deviations than with the previous dispersion solution (e.g. E140H-1526, see Fig. 17). These deviations were confirmed by an independent analysis of Ayres. After a series of tests which included verifying the A4CORR, SHIFTA2, and YREF terms in the new and previous CALSTIS (see Appendix), we realized that the larger deviations seen *only in some modes* could be due to the new set of lamp exposures utilized to compute the new coefficients for the dispersion solution. In the past, monthly MSM (Mode Selection Mechanism) offsets ($\sim$20 pixels) were applied regularly for STIS observations in order to uniformly age the MAMA detectors, meaning that the center of the spectrogram would fall on a different detector location then with the default zero offsets position which is used in recent observations. Indeed, we found that for those settings which presented the largest deviations in the new CALSTIS several lamp exposures were taken at large MSM offset positions (for instance for E140H-1526 the new coefficients were computed from 3 deep lamp exposures, the deepest of which was taken at MSM offset2 = -23 pixels). We are in the process of testing a new set of dispersion coefficients now derived using only deep lamp exposures taken at the default zero MSM offset position. This finding also led to the realization that there are not enough deep lamp exposures for all available modes to adequately improve upon the current wavelength solution (see Recommendations). In addition, we are testing a slightly different processing strategy in CALSTIS to better account for the spectral tilts seen in the wavecals with large y offsets (see Appendix for more details). This new procedure runs the wavecal processing twice for echelle data: the first cross-correlation between the lamp spectrum and the template spectrum finds the offset in cross-dispersion direction (SHIFTA2), then uses the computed SHIFTA2 in a second pass to apply the proper A4CORR. This last term is a coefficient in the CALSTIS dispersion model that compensates for spectral tilts which occur when the echelle pattern is offset in the y direction from the nominal position for that setting.

Conclusions

We analyzed high signal-to-noise wavelength exposures obtained after STIS was successfully repaired and resumed operations in May 2009 to test the wavelength accuracy of the CCD and MAMA modes. The settings obtained under programs PID 11858 and 11859 and analyzed here do not present any anomalous behaviors. The mean of the difference between observed and laboratory wavelengths, which is a measure of the accuracy of the wavelength zero point, is typically better than 0.1 pixels, as for pre-SM4.

Similarly, the standard deviation of the differences, a measurement of the relative wavelength accuracy, is typically better than 0.2 pixels. We have identified a few settings in which differences have higher order wavelength trends and might be improved using an expanded dispersion solution. Further tests are in progress.

Recommendations

We recommend to continue the yearly monitoring of the STIS CCD and MAMA dispersion solutions as an integral part of the long-term monitoring program. In addition, for the STIS MAMA echelle settings, additional deep engineering wavecal exposures could be acquired to improve the wavelength accuracy. A list of settings that would benefit from additional exposures is summarized in Table 3.

Change History for STIS ISR 2011-01

Version 1: 29 March 2011 - Original Document

References

Ayres, T. R. 2008, ApJS, 177, 626 **10**, 100
Kimble, R. A., Woodgate, B. E., Bowers, C. W. et al. 1998, ApJ, L492, 83 **10**, 100
Sansonetti, C. J., Kerber, F., Reader, J., Rosa, M. R. 2004, ApJS, 153, 555 **10**, 100
Wallace, L. & Hinkle, K. 2009, ApJ, 700, 720 **10**, 100

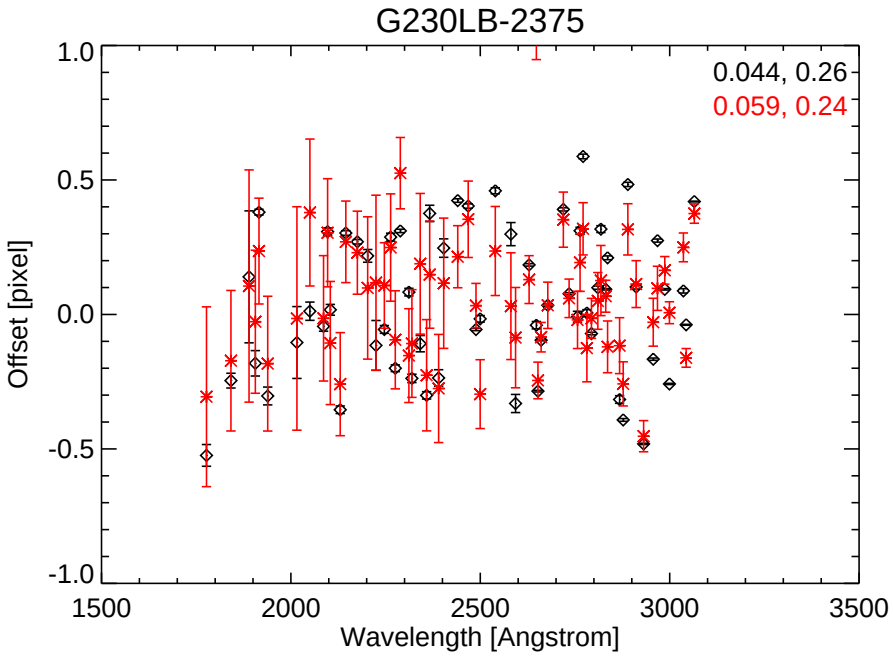

Figure 1. *Difference in pixels between observed and laboratory lines for the G230LB grating. Black diamonds are differences for centroids measured with gaussian fits to the observed lines while red asterisks for weighted mean centroids. The mean and standard deviation of the difference distributions are also given on the right upper corner in black for gaussian fits and in red for weighted mean centroids. One pixel corresponds to ∼175 km/s.*

Spectral Element	Central Wavelength [Å]	Recommended exposure [#×s]
priority 1: prime settings		
E140H	1416	3×1,000
E230M	2707	2×1,000
priority 2: secondary settings		
E140H	1453	2×1,000
E140H	1307	1×1,000
E230M	2269	1×1,500
E230H	2363	1×1,500
E230H	2263	1×1,500
E230H	2862	1×1,500
E230H	2663	1×1,500
E230H	1913	1×1,500
E230H	2413	1×1,000
E230H	2762	1×1,000
E230M	2561	1×1,000

Table 3. *Settings that would benefit from additional deep high signal-to-noise lamp exposures*

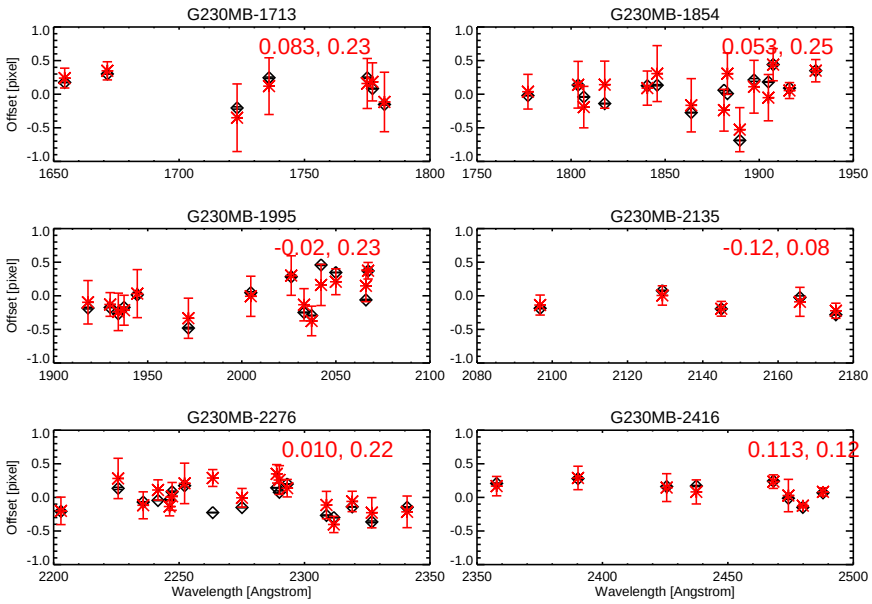

Figure 2. *Difference in pixels between observed and laboratory lines for G230MB gratings. Colors are as in Fig. 1. One pixel corresponds to ∼20 km/s at 2300 Å.*

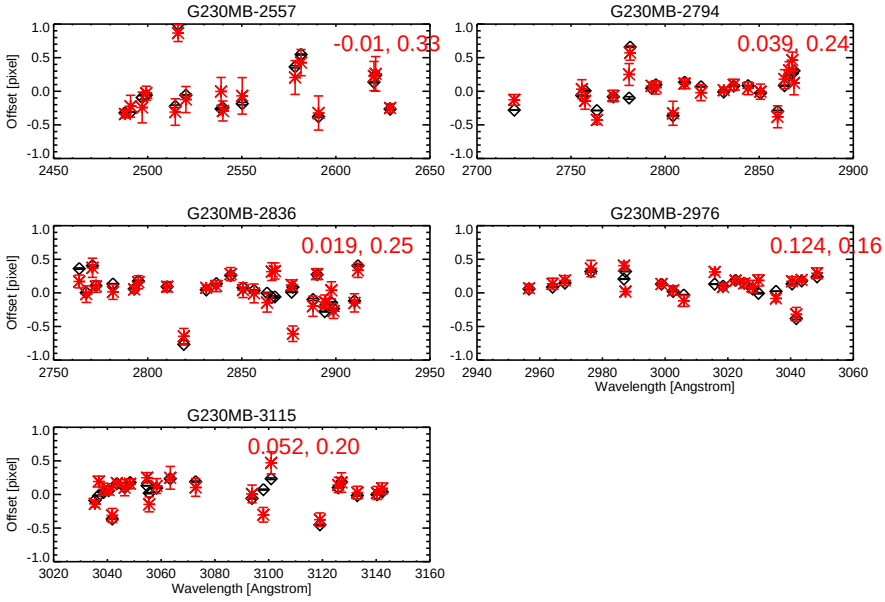

Figure 3. *Difference in pixels between observed and laboratory lines for G230MB gratings. Colors are as in Fig. 1. One pixel corresponds to ∼20 km/s at 2300 Å.*

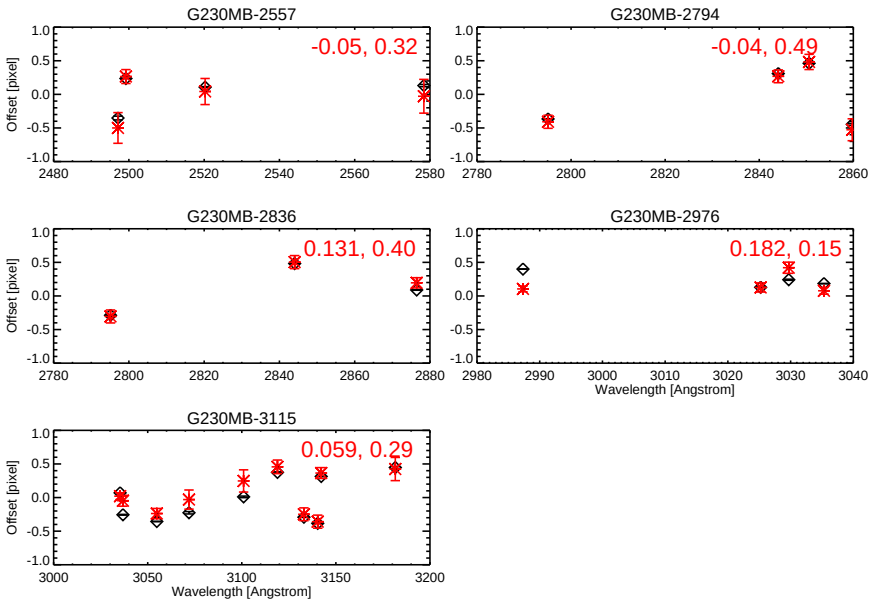

Figure 4. *Difference in pixels between observed and laboratory lines for G230MB gratings. This is the same as Fig. 3 but without the Wallace & Hinkle (2009) compilation of Cr I lines. Fewer lines are identified in these spectra. Colors are as in Fig. 1.*

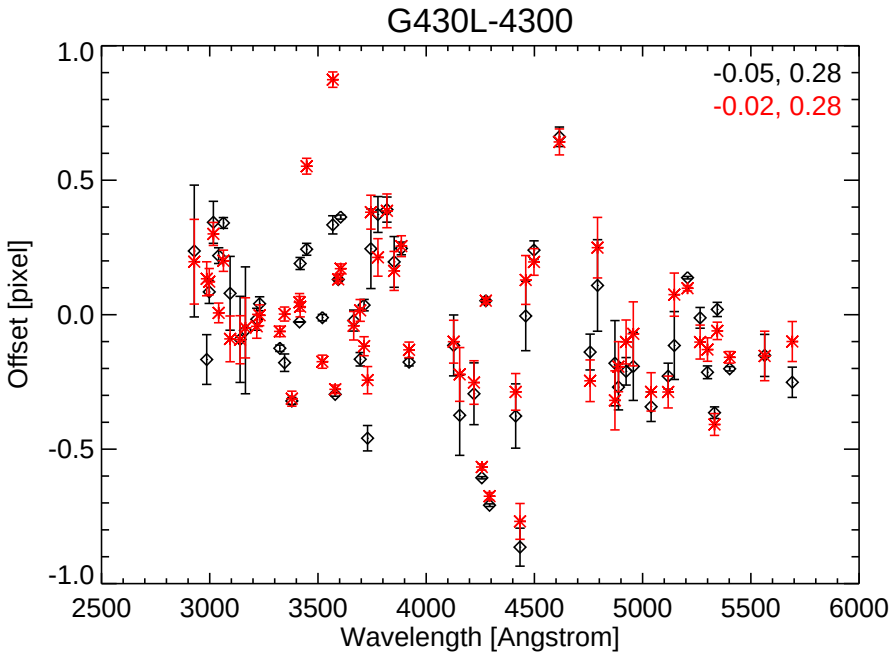

Figure 5. *Difference in pixels between observed and laboratory lines for the G430L grating (HITM1 lamp). Black diamonds are differences for centroids measured with gaussian fits to the observed lines while red asterisks for weighted mean centroids. The mean and standard deviation of the difference distributions are also given on the right upper corner in black for gaussian fits and in red for weighted mean centroids. One pixel corresponds to* $\sim$*240 km/s.*

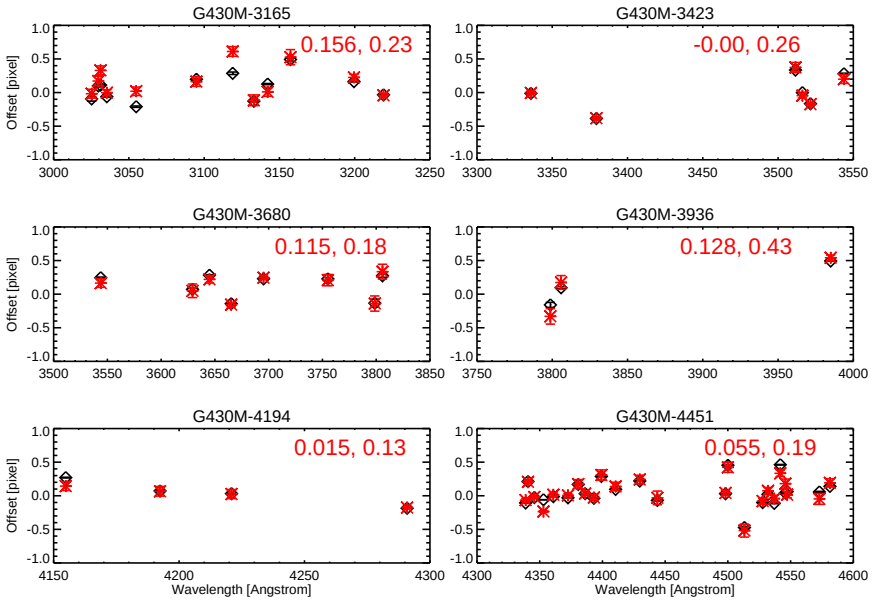

Figure 6. *Difference in pixels between observed and laboratory lines for G430M gratings. Colors are as in Fig. 5. One pixel corresponds to ∼25 km/s at 4300 Å.*

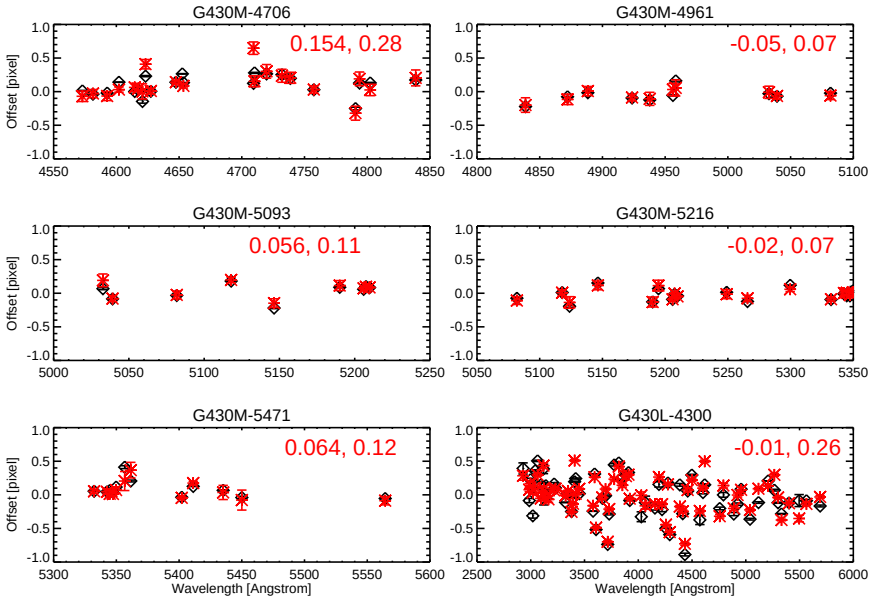

Figure 7. *Difference in pixels between observed and laboratory lines for G430M gratings except last panel where we show the G430L setting for the LINE lamp. Note that the difference distribution from this last panel is the same as that for the G430L HITM1 lamp setting (Fig. 5). Colors are as in Fig. 5. One pixel corresponds to* $\sim$*25 km/s at 4300 Å for the medium-resolution settings.*

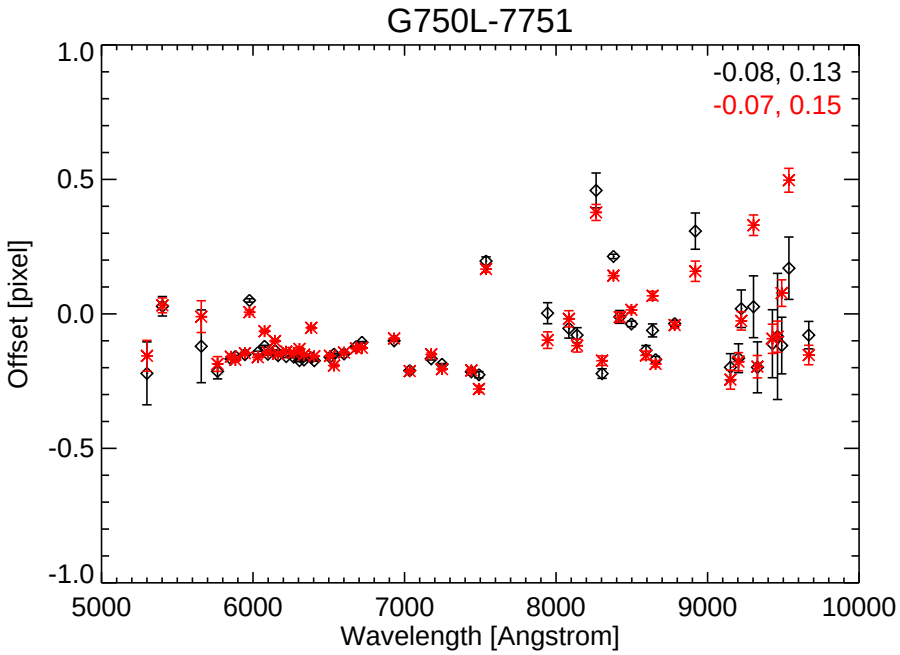

Figure 8. *Difference in pixels between observed and laboratory lines for the G750L grating. Black diamonds are differences for centroids measured with gaussian fits to the observed lines while red asterisks for weighted mean centroids. The mean and standard deviation of the difference distributions are also given on the right upper corner in black for gaussian fits and in red for weighted mean centroids. One pixel corresponds to* $\sim$*197 km/s at 7500 Å.*

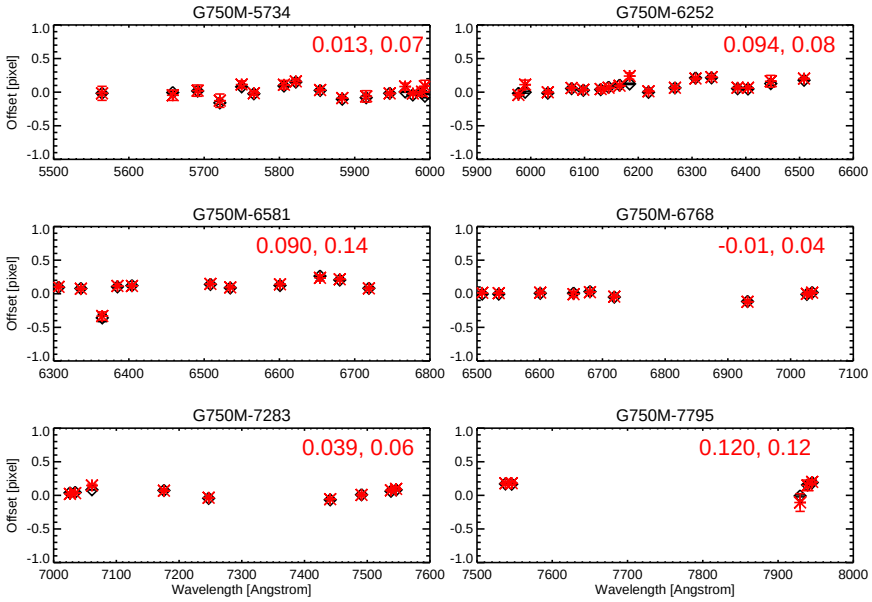

Figure 9. *Difference in pixels between observed and laboratory lines for G750M gratings. Colors are as in Fig. 8. One pixel corresponds to ∼22 km/s at 7500 Å.*

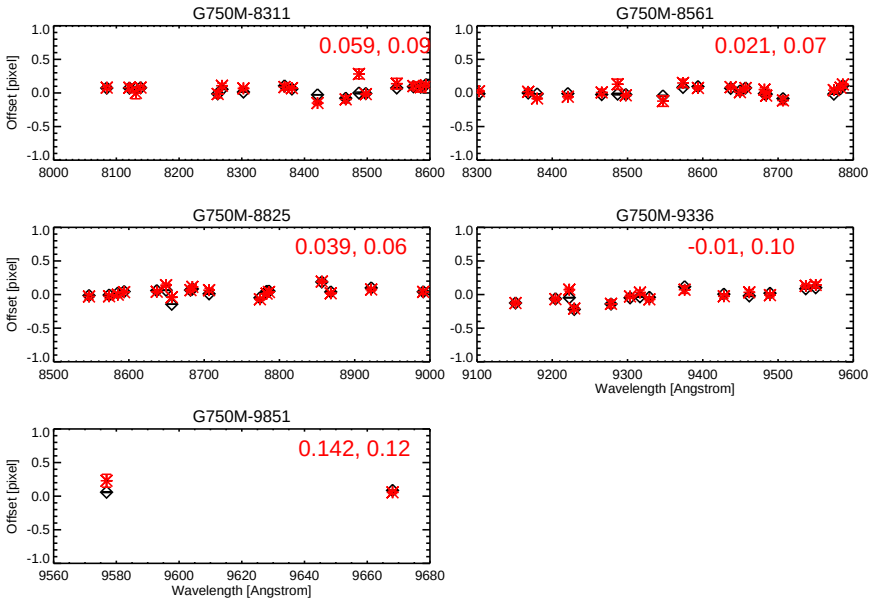

Figure 10. *Difference in pixels between observed and laboratory lines for G750M gratings. Colors are as in Fig. 8. One pixel corresponds to ∼22 km/s at 7500 Å.*

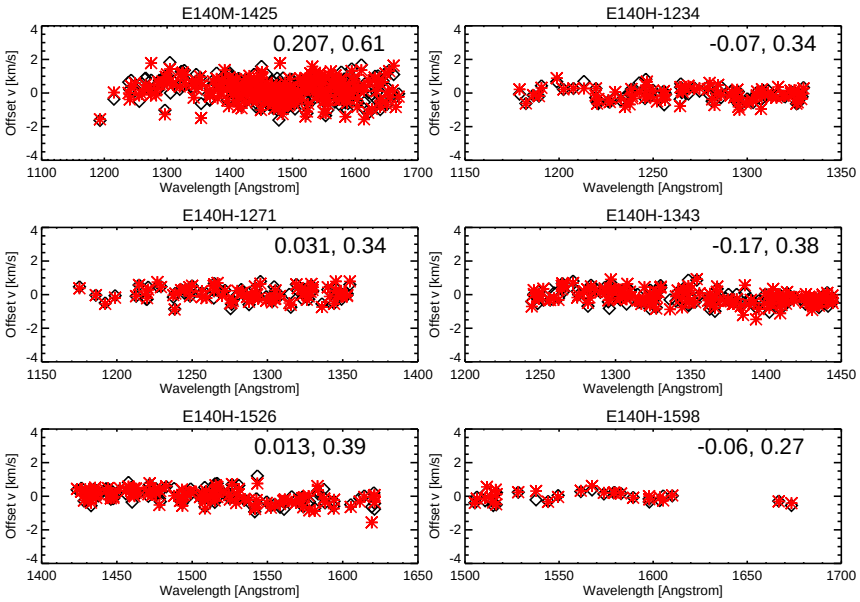

Figure 11. *Difference in velocity between observed and laboratory lines for the E140H and M gratings acquired within program PID 11859. The velocity scale is used to better compare these results with those reported by Ayres (2008). Black diamonds are differences for centroids measured with gaussian fits to the observed lines while red asterisks for weighted mean centroids. The mean and standard deviation of the difference distributions are also given on the right upper corner in black for gaussian fits. One pixel corresponds to* $\sim \lambda/228,000$ *Å or* $\sim$*1.3 km/s for the H settings and to* $\sim \lambda/91,700$ *Å or 3.3 km/s for the M settings.*

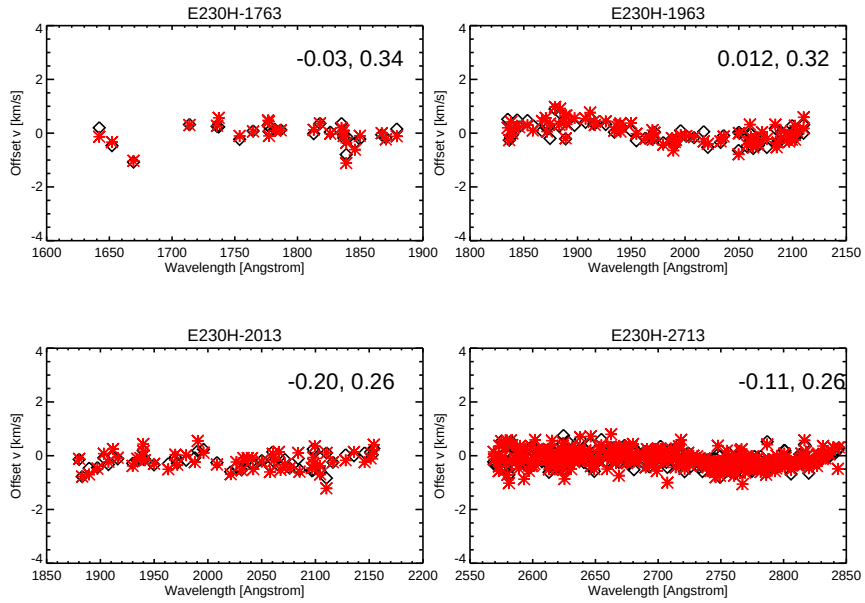

Figure 12. *Difference in velocity between observed and laboratory lines for the E230H gratings. Colors are as in Fig. 11. One pixel corresponds to* $\sim \lambda/228,000\,\AA$ *or* $\sim 1.3\,km/s$.

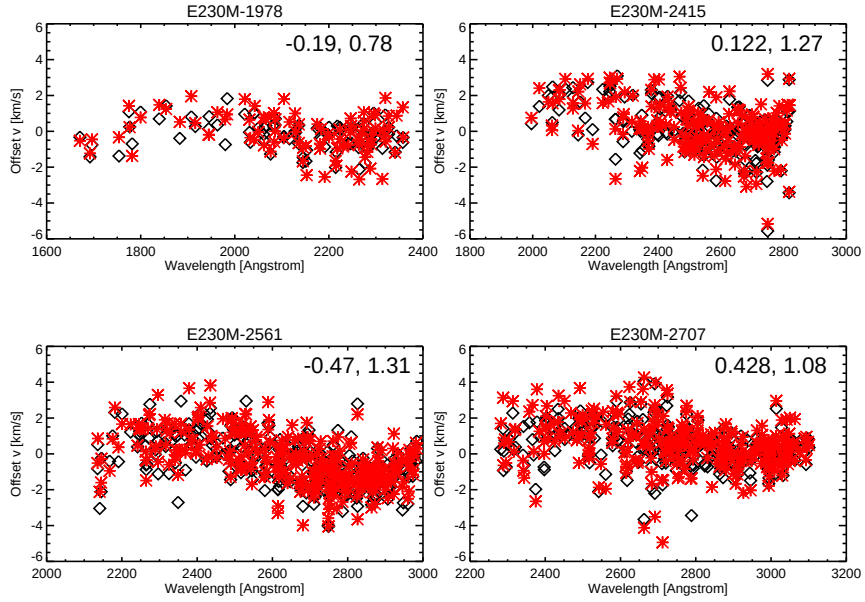

Figure 13. *Difference in velocity between observed and laboratory lines for the E230M gratings. Colors are as in Fig. 11. One pixel corresponds to* $\sim \lambda/60,000\,\AA$ *or* $\sim 5\,km/s$.

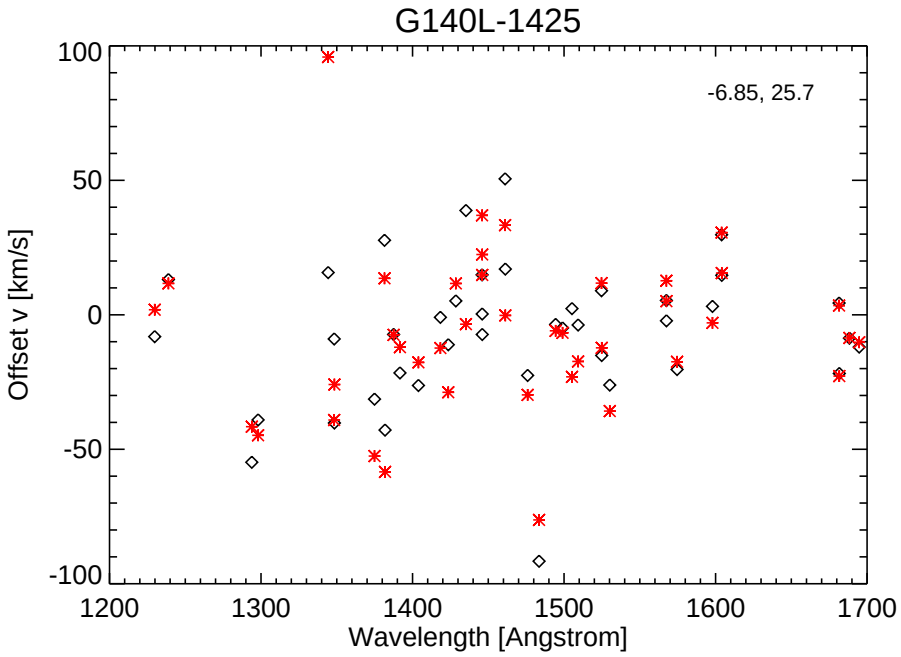

Figure 14. *Difference in velocity between observed and laboratory lines for the G140L grating. Colors are as in Fig. 11. One pixel corresponds to 0.6 Å or 126 km/s.*

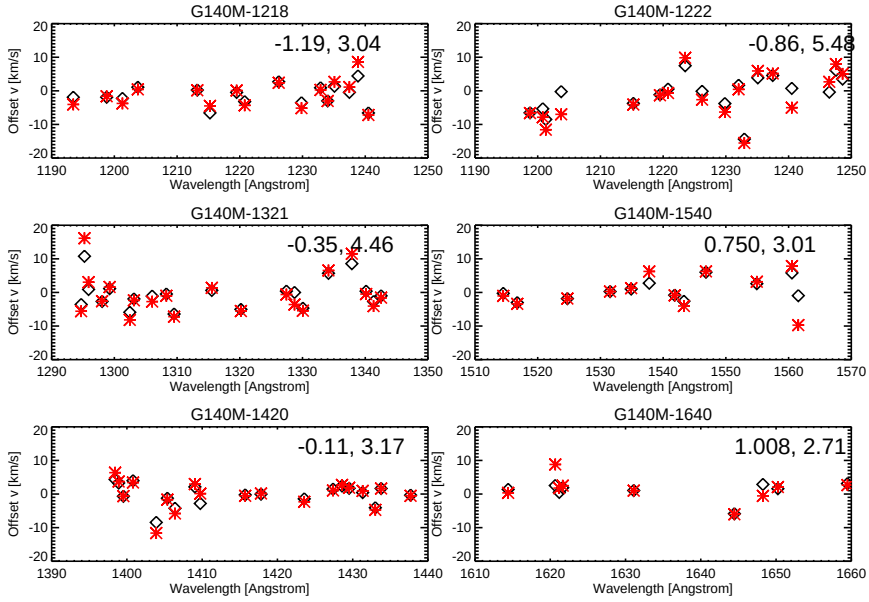

Figure 15. *Difference in velocity between observed and laboratory lines for the G140M gratings. Colors are as in Fig. 11. One pixel corresponds to 0.05 Å, about 10 times better than for the G140L setting.*

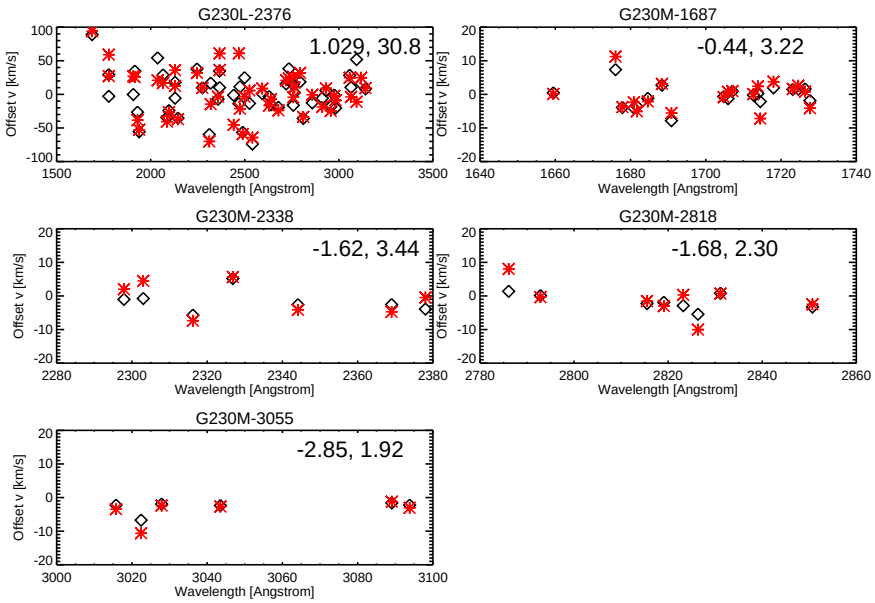

Figure 16. *Difference in velocity between observed and laboratory lines for G230L and M gratings. Colors are as in Fig. 11. One pixel corresponds to 1.58 Å (or 199 km/s) at the L setting and 0.09 Å for the M settings.*

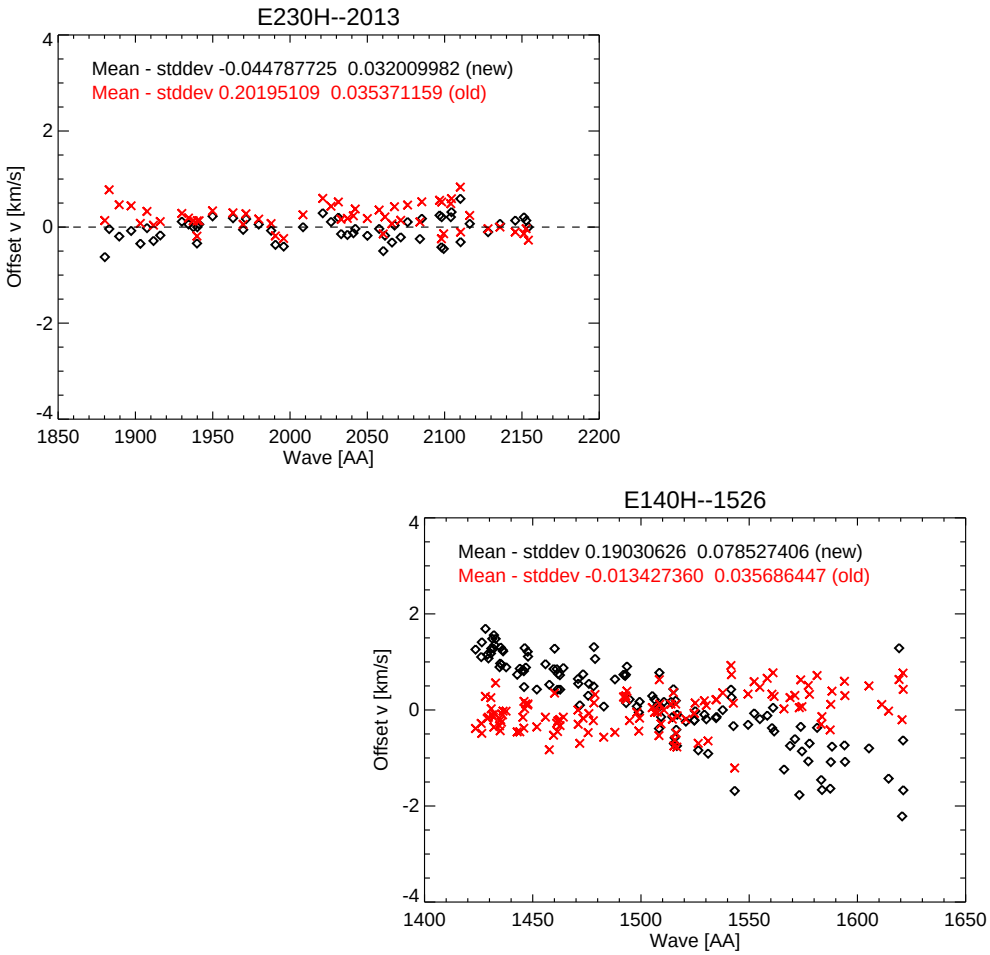

Figure 17. *Difference in velocity between observed and laboratory lines for two settings that have been processed with the new CALSTIS dispersion solution from T. Ayres. Black diamonds are differences using the new CALSTIS coefficients while red asterisks using the old coefficients. This wavelength solution resulted in an improvement between measured and observed lines for some settings (see upper panel) but not for all settings (see lower panel). The anomalous settings now have been recognized as those affected by wavecals taken at large y offsets. An improved approach is in progress to compensate self-consistently for those spectral tilts.*

Appendix

The image of the echelle spectra does not always fall at the same location on the detector. In early STIS data there was a deliberate offset to improve detector lifetime, and even now there will be a random offset of a few pixels in each axis. The offset in the cross-dispersion direction results in a small skew of the image, a shift in the dispersion direction that is directly proportional to the location in the cross-dispersion direction. This is called the A4 correction (A4CORR) because it is accounted for by modifying dispersion coefficients 0 and 4 (a0 and a4); the latter term is the one that depends only on wavelength. When the A4 correction was first added to CALSTIS there was a keyword that gave the approximate value of the offset in the cross-dispersion direction, and the value of that keyword was used in order to apply the A4 correction during wavecal processing. The correction is applied when constructing a template image; the shifts are determined by cross correlating the observed wavecal spectrum with the template. That keyword is no longer populated (it is set to zero), so calstis was recently modified to do the wavecal processing step twice, once to determine the offset in the cross-dispersion direction, then a second time with the A4 correction included, using the new y offset. The A4CORR, SHIFTA2, and YREF are linked to the a4 and a0 coefficients in the STIS wavelength dispersion solution as follows:

$$\mathrm{ydif} = \mathrm{ypos} - \mathrm{YREF} = \mathrm{SHIFTA2} + \mathrm{a2center} - \mathrm{YREF}$$

$$\mathrm{a4} = \mathrm{a4} + \mathrm{A4CORR} \times \mathrm{ydif}$$

$$\mathrm{a0} = \mathrm{a0} - \mathrm{cenwave} * \mathrm{A4CORR} * \mathrm{ydif}$$

where a2center is taken from the trace table (SPTRCTAB) for spectral order MREF. YREF is the location of order MREF in the WAVECAL used to determine the dispersion coefficients. (ypos - YREF) is the global offset of the lamp image in the Y direction with respect to the template lamp image.